Journal of Industrial Microbiology & Biotechnology (1999) 23, 155–165

http://www.stockton-press.co.uk/jim

Protein diffusion in alginate beads monitored by confocal microscopy. The application of wavelets for data reconstruction and analysis

A Laca[1], LA García[1], F Argüeso[2] and M Díaz[1]

[1]*Dept of Chemical Engineering and Environmental Technology (IUBA), University of Oviedo, c/Julián Clavería s/n, 33071 Oviedo, Spain;* [2]*Dept of Mathematics, Faculty of Sciences, University of Oviedo, c/Calvo Sotelo s/n, 33007 Oviedo, Spain*

A microscopic technique has been developed to obtain the protein profiles inside calcium alginate gel. To do this, the diffusion of BSA, previously marked with FITC, inside calcium alginate beads was observed using confocal laser microscopy, thus obtaining the spatio-temporal evolution of the protein concentration. The technique, however, presents certain limitations and zones where it is impossible to obtain experimental data. Wavelets analysis, commonly used in signal processing and statistics, was employed to reconstruct and subsequently analyse the experimental results. Once the diffusion model was defined, the substrate profiles obtained were used to calculate a diffusivity value for BSA in alginate gel.

Keywords: diffusion; BSA; alginate; wavelets

Introduction

Analysis of the different uses of immobilized cell systems and their modelling has been an important area of study throughout the last decade [2,17,25,26,28], mainly due to the advantages that these systems present in contrast with cell-free systems [22]. When working with immobilized systems, we have to know the diffusional properties of the species involved, since diffusion can be the main cause of limited cell growth during a fermentation process [25,26,28], and also the specific phenomenon that controls the release of products to the external liquid medium. For this reason, many authors have studied the diffusion of substrates through different immobilization supports, in particular alginate and other polysaccharide gels [15,19,23,24].

In some cases small solutes ($<$20 000 D) can diffuse as freely into alginate gel beads as into water [24], or with a slightly lower effective diffusivity than that in water [19]. However, controversy arises when regarding larger solutes ($>$65 000 D). Tanaka *et al* [24] stated that these solutes are not able to diffuse from the liquid medium towards the inside of the immobilization support. On the other hand, Shoichet *et al* [23] calculated the diffusivity values of BSA and immunoglobulin through alginate when penetrating into the support from the liquid medium.

Diffusivity properties in alginate are influenced by a great number of factors [15,19,24]: the concentration and composition of the alginate, the conditions of support preparation, pH and temperature. The number of alginate-calcium bridges decreases with time and hence permeability with respect to the solutes increases [23]. Likewise cells growing in the support can influence the diffusional process [2,17,28], causing a decrease in the substrate's ability to diffuse through the support.

Studies of *Serratia marcescens* immobilised in alginate and fermenting whey [12,20] led to the need to ascertain the diffusional behaviour of the whey proteins in this system. With this in mind, we chose one of the larger proteins, BSA (69 000 D, 0.3–0.6 g L^{-1} in whey) [7]. Most of the diffusional studies were carried out by monitoring the species concentration in the liquid medium and the subsequent application of a diffusion model [19,23,24]. Martinsen *et al* [15] sectioned beads containing [^{14}C]-albumin, and determined the concentration profile inside them by scintillation counting.

In the present work, and in order to obtain these profiles over time, confocal laser microscopy was employed, of the protein labeled with fluorescein isothiocyanate (FITC). The concentration profiles obtained allowed us to select an adequate diffusion model to obtain BSA diffusivity through the alginate. However, there are difficulties in obtaining BSA concentrations in some zones, which require a method that allows analysis and reconstruction of the results. The method chosen in this case for data treatment was that of wavelets.

Wavelets [9,18] constitute a refinement of Fourier analysis and have been useful for analysing and de-noising signals and images, substantially reducing contaminating noise. In statistical analysis, these methods are also employed for reducing random errors made when measuring and reconstructing the original data. In the present case, wavelets were employed to de-noise the gross data, eliminating Gaussian errors, to study the goodness of fit of these data to theoretical model equations, and finally allowing us to differentiate fluctuations due to Gaussian or systematic errors.

Correspondence: M Díaz, Dept of Chemical Engineering and Environmental Technology, Faculty of Chemistry, University of Oviedo, C/Julián Clavería s/n, 33071 Oviedo, Spain
Received 9 February 1999; accepted 14 May 1999

Experimental methods

Preparation of alginate beads [27]

Sodium alginate (Janssen Chimica, Geel, Belgium) (2.1% w/v) was allowed to drop at a constant rate into a solution of $CaCl_2$ (3% w/v) that was continuously agitated. The beads remained in the $CaCl_2$ solution for 30 min, completing the alginate gelling process. The beads obtained in this way had an average diameter of 3.1 ± 0.2 mm and a dry weight of 35 mg ml^{-1}.

Protein labeling with FITC [8]

Ten per cent of a BSA solution (8 mg ml^{-1}) [12] was labeled and later re-mixed with the rest of the solution in order to avoid a modification of its properties. Ten milliliters of the BSA solution were dialysed (dialysis tubing D-9777) *vs* 500 ml of FITC labelling buffer (0.05 M boric acid, 0.2 M NaCl, pH adjusted to 9.2 with NaOH), at 4°C, changing the buffer three times in 2 days. Subsequently, 20 μl of FITC solution in dimethyl sulfoxide (5 mg ml^{-1}) were added for each mg of protein and this new solution was

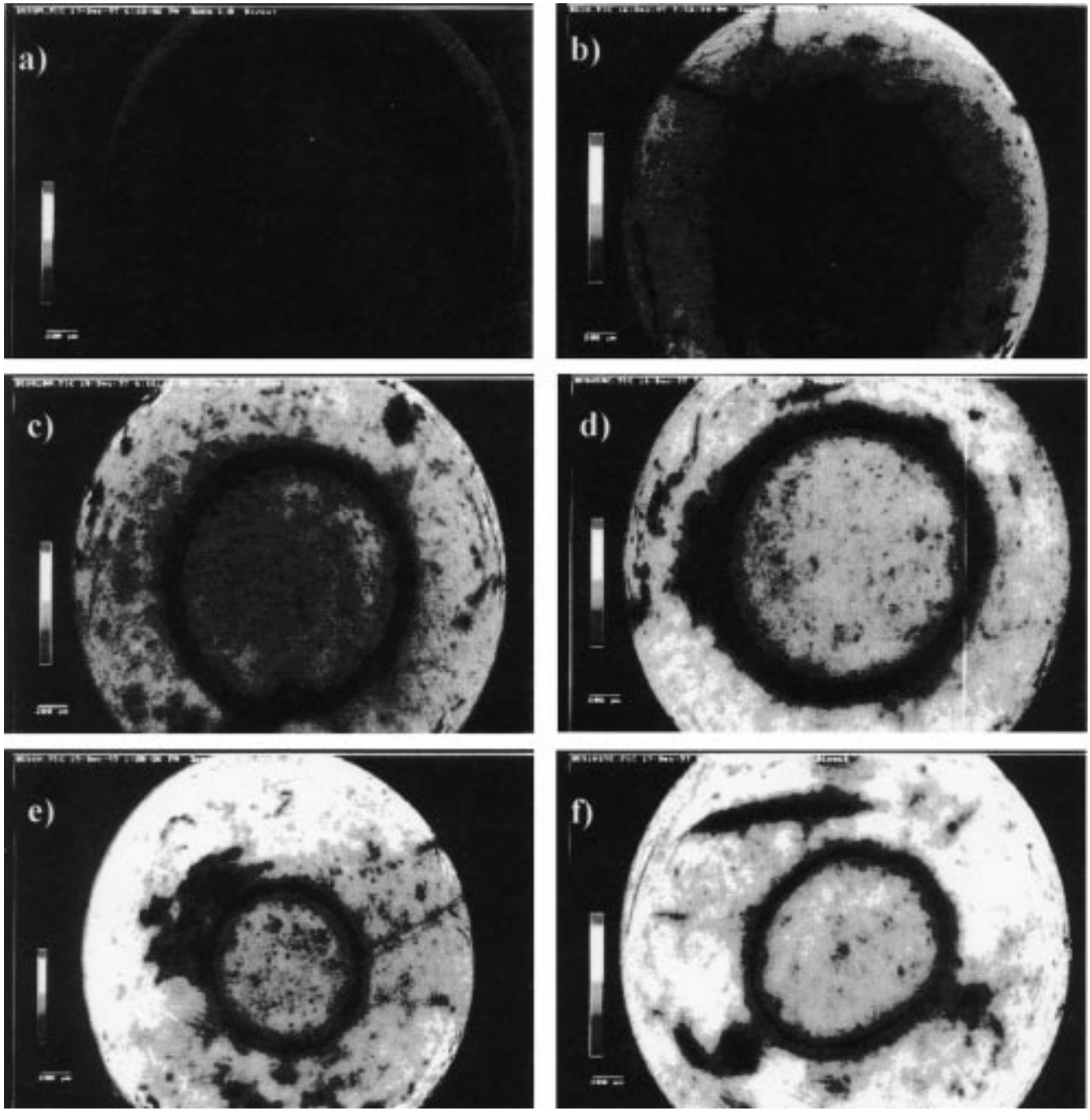

Figure 1 Central sections of alginate beads at different diffusion times (confocal laser microscopy). (a) 35 min; (b) 1 h; (c) 3 h; (d) 5 h; (e) 16 h; (f) 51 h.

incubated for 2 h at room temperature. Excess FITC solution was eliminated by dialysis *vs* 500 ml of the dialysis buffer (0.1 M tris Cl (pH 7.4), 0.1% (w/v) NaN_3, 0.2 M NaCl, pH adjusted to 7.4 with HCl).

Diffusion experiments

Alginate beads were introduced into flasks in such a way that the beads were covered by the partially-labeled BSA solution to allow the protein to diffuse through the internal part of the beads by incubating the flasks in an orbital shaker at 150 rpm, 4°C, and in darkness. The beads were kept under these conditions for different times, and after being lightly dried with filter paper, were ready for analysis using confocal microscopy.

The beads were then dissolved in 1% (w/v) sodium citrate (1 g of beads in 10 ml of solution) with agitation. The total amount of protein released into the solution was analysed by the Lowry procedure [13].

Confocal microscopy

A confocal laser microscope (BIO-RAD MCR 600) with a BHS filter was used. This technique offers the possibility of observing the zones of support reached by the labeled protein, and it is possible to analyse sections of the sample without making cuts in the beads that could damage them. The images obtained were analysed using the COMOS and SOM software, THRU-VIEW.

In spite of the advantages that the confocal microscopy technique offers [14], difficulties also arise:

- The microscope presents a series of parameters (black level, gain, diaphragm, laser intensity) that must be fixed by the operator. The values of these parameters were fixed at the beginning and kept constant throughout the observations.
- Photographs must be taken immediately since the exposure time can affect the results (photobleaching [4]); hence, they were always taken after the first laser scan.
- When observing the central sections of beads exposed to the labeled protein for a long time, the presence of a dark crown was detected just around this central zone (Figure 1). This crown is wider the wetter the bead is, which confirms that it is an artefact caused by the bead having to rest on a Petri dish in order to be observed. Thus, water drips through the lower parts, forming a ring around the contact point between the bead and the support. The laser ray collides with this ring, which impedes it from reaching every point of the sample with the same intensity, causing the dark zones that appear in the photographs. Therefore, a light drying of the beads was carried out to minimise the effect, since a total drying would degrade their structure. The data corresponding to these dark zones were interpolated.

Besides these problems inherent in microscopic observations, other error-including effects have to be mentioned:

- The time from the extraction of the beads to observation under the microscope contributes to the error because the protein will continue to diffuse inside the support. This time lapse was as short as possible (≈5 min) and the same in all cases.
- A drop in protein concentration on the border of the beads was detected due to the drying process, which means that the data in this zone must be reconstructed.
- The structure of the gel matrix that constitutes the alginate beads may present inhomogeneities [11]. Thus, weaker gelling zones or microvoids could lead to differences in protein diffusion and asymmetry.

All these effects could lead to results that are not considered in the model, because of complex real structures or systematic errors. Moreover, the measuring system itself (microscope, image analysis equipment) provides data with point to point fluctuations, causing Gaussian errors.

Mathematical analysis

In recent years, there has been a widespread application of wavelets analysis to mathematical treatment of data, signals and images in a variety of scientific areas ranging from medicine and biology [1] to electromagnetism [10] or astrophysics [21]. Wavelets are a refinement of Fourier analysis; whereas Fourier analysis allows us to expand a periodic function as a sum of trigonometric functions (a sum of waves with different frequencies), wavelets include a new ingredient: localisation.

If we consider experimental data represented by a certain function $f(x)$, we can analyse these data using wavelets, taking into account its structure at different levels of resolution; this resolution being able to change from point to point. A number of basic concepts concerning wavelets are defined next. A mother wavelet $\psi(x)$ and a scaling function $\phi(x)$ are unidimensional functions satisfying suitable mathematical properties [9,18]. Wavelets $\psi_{j,k}$ and scaling functions $\phi_{j,k}$ are constructed from ψ and ϕ through dyadic dilations and translations.

$$\psi_{j,k} = 2^{j/2}\psi(2^j x - k) \tag{1}$$

$$\phi_{j,k} = 2^{j/2}\phi(2^j x - k) \tag{2}$$

where j and k are integers. The index j labels the level of resolution and k fixes the position. Given a function $f(x)$, approximation coefficients $c_{j,k}$ and detail coefficients $d_{j,k}$ are defined as

$$c_{j,k} = \int f(x)\phi_{j,k}(x)\mathrm{d}x \tag{3}$$

$$d_{j,k} = \int f(x)\psi_{j,k}(x)\mathrm{d}x \tag{4}$$

If we are dealing with N data $N = 2^J$ (J an integer) and assume the data take values $f_J(x_i)$ constant in equally spaced subintervals of [0,1] (the method can be extended to more general cases), we can expand the function $f_J(x_i)$ at any data point x_i as:

$$f_J(x_i) = f_{J-1}(x_i) + g_{J-1}(x_i) \tag{5}$$

where f_{J-1} is called the first level approximation and g_{J-1} the first level detail and are given by $(1 = 2^{J-1} - 1)$

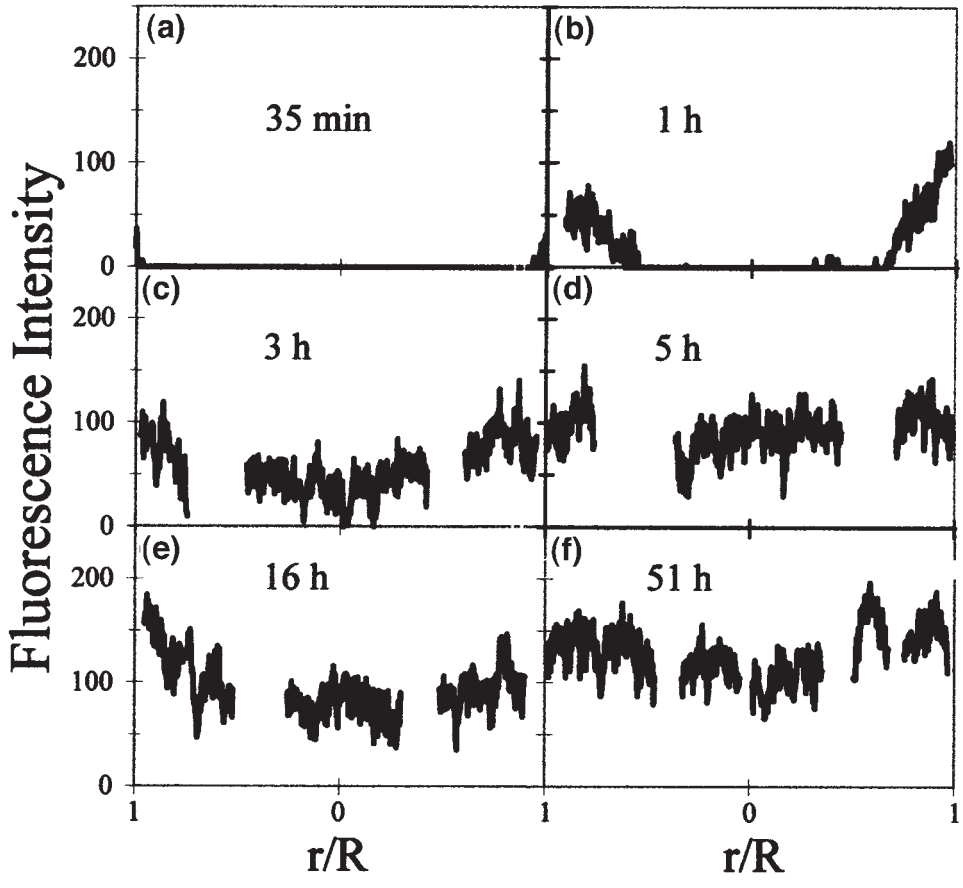

Figure 2 BSA fluorescence intensity profiles in alginate beads (r/R = dimensionless radius) at different diffusion times. (a) 35 min; (b) 1 h; (c) 3 h; (d) 5 h; (e) 16 h; (f) 51 h.

$$f_{J-1}(x_i) = \sum_{k=0}^{1} c_{J-1,k}\phi_{J-1,k}(x_i) \tag{6}$$

$$g_{J-1}(x_i) = \sum_{k=0}^{1} d_{J-1,k}\psi_{J-1,k}(x_i) \tag{7}$$

f_{J-1} can also be written as a sum of second level approximation f_{J-2} and second level detail g_{J-2}. This can be repeated till f_J can be finally written as:

$$f_J(x_i) = c_{0,0}\phi_{0,0}(x_i) + \sum_{j=0}^{J-1}\sum_{k=0}^{2^j-1} d_{j,k}\psi_{j,k}(x_i) \tag{8}$$

As j increases from zero to $J-1$, the wavelets represent the structure of the function on increasingly smaller scales, with each scale a factor 2 finer than the previous one. The index k denotes position.

From a practical point of view, the first level approximation means an 'average' of two successive data, whereas the first level detail represents the difference of this average with respect to the original data. If we decrease the resolution, going to lower values of j, we are considering 'averages' of 2^m data, where m is the approximation level. The details give the difference between two successive levels of approximation.

If we assume that our data are affected by Gaussian errors with mean zero and standard deviation σ (noise-in-signal theory), the detail coefficients at the first level will be dominated by the noise and can be used to estimate σ through their standard deviation or other more robust estimators [18]. We can also cut down the errors in a significant way by using a technique called 'soft thresholding'. This technique consists in fixing a suitable threshold λ, setting all the detail coefficients $d_{j,k}$ with absolute values lower than λ to zero and replacing those higher than this value by $\delta_{j,k}$ with

$$\delta_{j,k} = d_{j,k} - \lambda \quad (\text{if } d_{j,k} > \lambda) \tag{9}$$

$$\delta_{j,k} = d_{j,k} + \lambda \quad (\text{if } d_{j,k} < -\lambda) \tag{10}$$

We use the universal threshold [6] $\lambda = \text{sqrt}(2 \log N)\,\sigma$, where σ has been previously estimated and N is the data number ($N \cong 500$ in our case). In this way, the errors are subtracted from the coefficients $d_{j,k}$ and the new coefficients $\delta_{j,k}$ are used to reconstruct the denoised data by means of Eqn 8. Since the contribution of the noise in our data is only significant till level 5, we perform the denoising only until that level. Different families of wavelets can be used in this process. The Daubechies 4 wavelets [5] proved to be very efficient for denoising. We used the MATLAB WAVELET TOOLBOX [16] for analysis and denoising

process. This toolbox is also adequate for compressing one-dimensional signals and two-dimensional images.

Results and discussion

Result forms

Some pictures corresponding to central zones of the support obtained by confocal microscopy are shown in Figure 1. In these pictures, the protein penetrates into the interior of the support (greater fluorescence intensities, higher protein concentration), reaching the centre of the sample after diffusion. After 16 h, it is not possible to observe any increase in fluorescence, so it is approximately at this moment when the beads are considered to be saturated with protein.

In these pictures, we have selected some directions crossing the beads in a random way. Based on the fluorescence intensity, the data analysis program gives an intensity number at certain points along the diameter. Three directions were analysed in each of the pictures, but only one of the profiles for each time is shown in Figure 2, as an example. In these graphs, it is possible to see more clearly how the protein enters the support, initially only in the surface areas and later in the central zones, concave profiles appearing that develop with time.

Result tests

In order to validate the microscopic method employed, the total amount of protein in the support was analysed at different times. The results are shown in Figure 3(a). One can observe the rapid entrance of the protein in the alginate support at the beginning of the diffusion process, which continues more slowly until it reaches the saturation point at 16–20 h, which confirms the microscopy data. The maximum concentration of BSA in the support is 5.8 mg ml^{-1} of support. The comparison of these values with those obtained by the microscopic technique allows us to obtain an equation, which will be presented later, relating fluorescence intensity and BSA concentration.

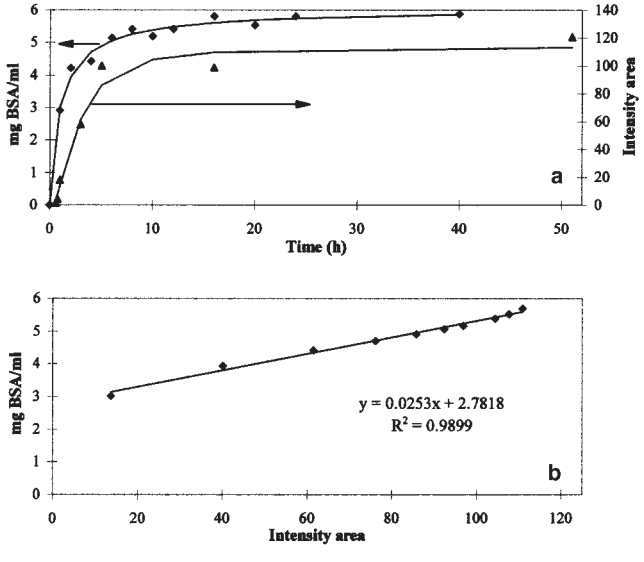

Figure 3 (a) Total BSA concentration and fluorescence intensity area *vs* diffusion time: experimental (symbols) and interpolated (lines) data. (b) Relationship between total BSA concentration and fluorescence intensity area.

Analysis of results

Denoising gross data with wavelets: Gross data are a mixture of the 'original' data and random-type errors. When reconstructing the original data, wavelets analysis is of extraordinary value, since it allows us to carry out a process denominated denoising, that consists in suppressing the local random errors (noise) and recuperating the original data (signal). Wavelets do not require a previous data fitting model.

It is assumed that random errors present a Gaussian distribution with a zero mean and standard deviation σ. Because only one measurement for each point, time and direction was made, σ may not be calculated. In this case, wavelets offer an alternative method for determining σ. Detail coefficients of the first level are dominated by local random errors (noise in signal theory) and σ may be estimated by means of the standard deviations of the detail coefficients of the first level (local fluctuations). When working with Gaussian simulations, this estimation method gives excellent results. In accordance with this estimation, σ values are obtained (Table 1) of 10–12 order (σ is considered the same for every point in the space, although varying with time and direction).

The detail coefficients are analysed at different levels in order to eliminate noise. The first levels, including the third, are dominated by the noise and are therefore eliminated from the process. Noise is normally eliminated until the fifth level, where a mixture of signal and noise still appears; the method used being soft thresholding, as was explained in the mathematical analysis. Gaussian simulations added to signals were carried out, where $\sigma \cong 10$ normally passes to $\sigma \cong 2$, which implies a significant reduction in the noise when employing this technique.

The signals reconstructed with this method are shown in Figure 4(c) and (f), for 3 h (two directions) and 51 h (one direction). In these figures, it can be observed that the clean data obtained suggest a parabolic-type fitting. This type of fitting might be adequate from a physical point of view of the system, since when protein diffuses, it first reaches the external zones of the support, subsequently diffusing through the internal parts. This means that even when the protein reaches these central zones of the beads, its concentration is lower there than in the more external zones.

In every case, Daubechies 4 was used as the type of wavelets, similar results being obtained when working with other Daubechies bases with a higher N. Because of the fragmentary character of the data, the reconstruction is sometimes not very good at the extremes. When Gaussian simulations of fragmentary data are carried out, reconstruction only presents small problems at the extremes, that hardly affect the complete data.

Parabolic fitting and modelling

Based on the fluorescence intensity data and as the disposition of those data suggests, results were fitted to a symmetric parabola with respect to the centre of the support, $x = 0.5$; denoting the fluorescence intensity by y and the

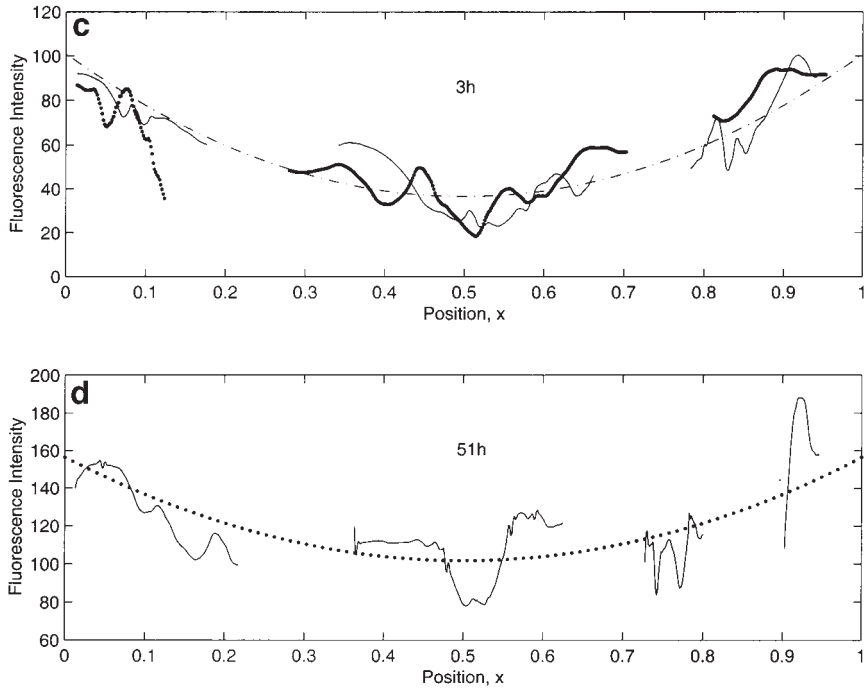

Figure 4 Fluorescence intensity data denoised by wavelets and parabola fitting *vs* position in the bead at two different diffusion times. (c) 3 h (solid and dotted line: data denoised in two random directions; dash-dotted line: fitting parabola). (f) 51 h (solid line: data denoised in one random direction; points line: fitting parabola).

Table 1 Gaussian and systematic deviations

Time (h)	Directions	σ	σ_s
1	1	10.3	12
	2	8.6	19
	3	10.2	11.5
3	1	10.6	13.5
	2	9.9	18.7
	3	10.3	12
5	1	10.8	15.6
	2	11.5	12.9
	3	9.8	13
16	1	10.5	24
	2	10.2	23.3
	3	12.2	16.8
51	1	11.4	20.8
	2	11.7	26.9
	3	9.5	20.6

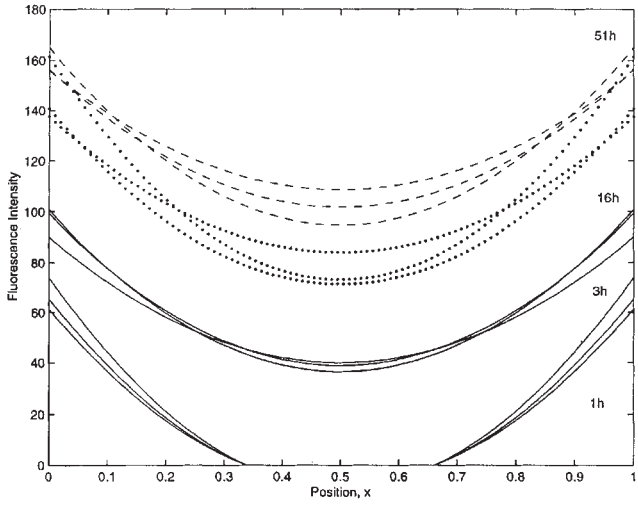

Figure 5 Parabolic fitting at different diffusion times.

position by x. Fitting to $y = a(x^2 - x) + b$ or $y = az + b(z = x^2 - x)$ was carried out for the three directions in which measurements were made and also for the different times assayed; coefficients a and b and the corresponding parabolas are shown respectively in Table 2 and Figure 5.

The area under the parabola of the fitting (intensity area) is obtained for each time assayed and the mean values are shown in Figure 3(a). This area under the fitting curve will correspond to the area under the curve resulting from joining gross data. This is because the mean of the gross data will be equal to the mean of the data supplied by the fitting curve calculated by square minima, so when integrating data under the curve, the result will be the same in both cases.

The values shown in Figure 3(b) are obtained by interpolating the data obtained by calculating the areas and those of the total amount of protein inside the support obtained by the Lowry method and comparing them. When protein concentrations are between 3.0 and 6 mg BSA ml^{-1}, corresponding to 1–20 h, both types of values can be related by a straight line [Figure 3(b): BSA (mg ml^{-1}) = 0.0253 × Intensity + 2.6942] that allows the profiles of fluorescence intensity to be transformed, in an approximate way, into profiles of protein concentration. This relationship can not be extrapolated to lower times because a minimum protein

Table 2 Fitting parameters: $y = az + b$; $z = x^2 - x$

Time (h)	Directions	a	b
1	1	291.9	65.4
	2	330.1	73.9
	3	273.4	61.3
3	1	242.6	99.5
	2	201.1	90.2
	3	257.5	100.9
5	1	85.1	105.9
	2	195.5	140.8
	3	111.1	118.7
16	1	353.3	161.4
	2	214.2	137.5
	3	277.8	140.8
51	1	189.4	155.9
	2	281.2	165
	3	218.9	156.5

concentration value needs to exist inside the support in order to be detected using the microscope. For shorter times, the zones where no fluorescence is observed are greater, although a certain amount of BSA may exist, always lower than 3 mg ml^{-1}. Besides, when interpolating data, only a little were available at these early times, being zones of high slope, so a slight deviation will lead to a large error when establishing the correlation.

The parabolic profiles obtained suggest analogous behaviour to that of applying the homogeneous diffusion model used in previous works [12,15] to modelize these alginate systems:

Mass balance inside the support:

$$\frac{\partial C_s}{\partial t} = \frac{1}{r^2}\frac{\partial}{\partial r}\left(r^2 D_s \frac{\partial C_s}{\partial r}\right) \tag{11}$$

Mass balance in the reactor:

$$\frac{dC_{bs}}{dt} = -\frac{3}{R}\frac{(1-\varepsilon_L)}{\varepsilon_L} D_s \frac{\partial C_s}{\partial r}\bigg|_{r=R} \tag{12}$$

where C_s is the protein concentration in the support and D_s the diffusivity of the protein in the support, r the radial coordinate of the support, R is the average radius of the spherical particles, C_{bs} the protein concentration in the liquid medium and ε_L the porosity of the bed. The values employed in the simulation were $\varepsilon_L = 0.73$ and $R = 0.00155$ m.

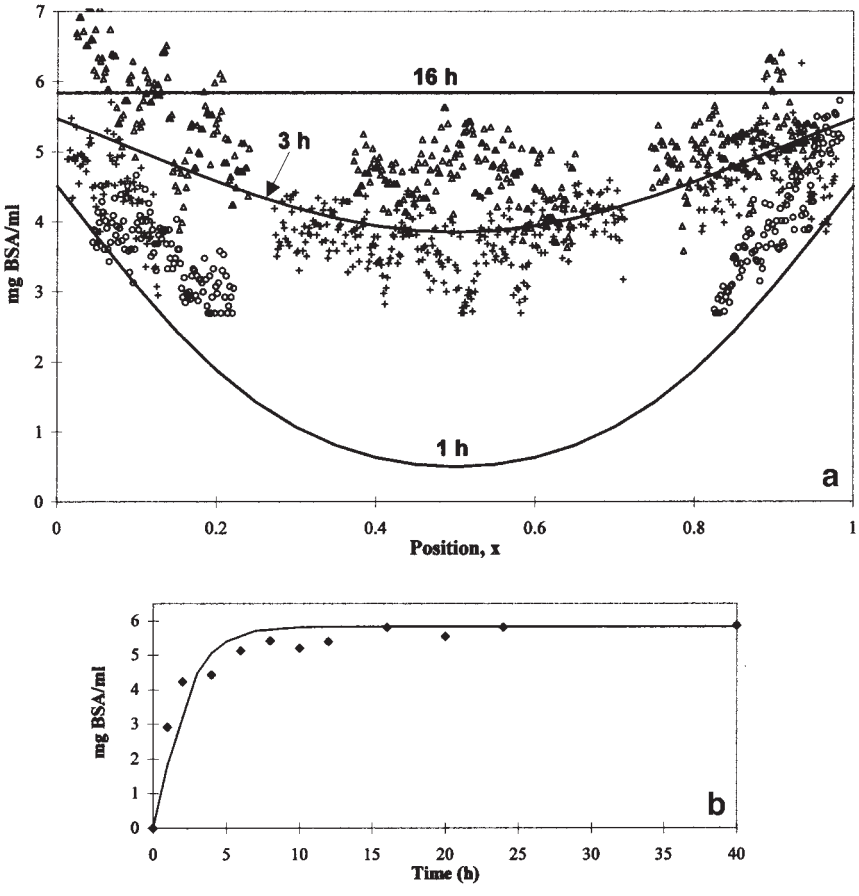

Figure 6 (a) Simulated (solid lines) and experimental (symbols) BSA concentration profiles in alginate beads, coming from fluorescence intensity profiles, at different diffusion times: (○) 1 h; (+) 3 h; (△) 16 h. (b) Simulated (solid line) and experimental (symbols) total BSA concentration *vs* diffusion times.

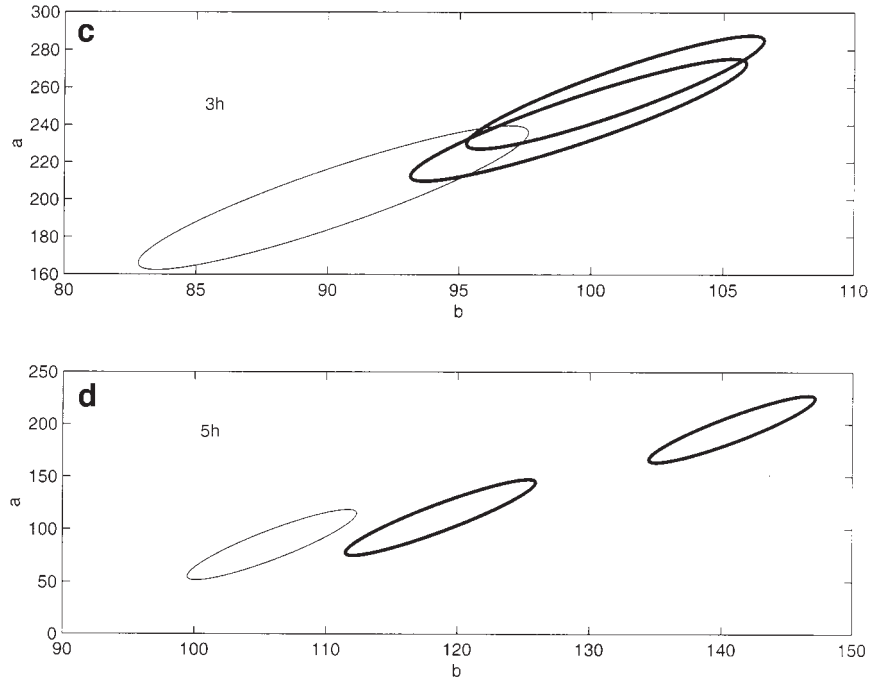

Figure 7 Outlines of probabilities at a 99% level in three random directions at two different diffusion times. (c) 3 h; (d) 5 h.

The protein concentrations on the surface of the support are different from the liquid medium protein concentrations at each moment so that it is necessary to employ an external resistance in the model. Hence, an external resistance was introduced using the boundary conditions presented in a previous work [12] ($K = 1935\ m^{-1}$).

$$r = R, \quad \frac{\partial C_s}{\partial r} = K(C_{bs} - C_s(R)) \tag{13}$$

where K is a mass transfer coefficient in the external film. Its presence may be due to two reasons: the existence of a real external film surrounding the beads caused by a low degree of agitation in the liquid medium or to a dense 'membrane' of very high alginate concentration found [3,15] on the support surface that could hinder the entrance of the protein and that we assume to be similar to an external film [12]. Of course, both phenomena could take place at the same time.

The value of the diffusion coefficient of BSA in alginate gel beads determined by employing the model was $5.5 \times 10^{-7}\ cm^2\ s^{-1}$. This value is within the range of the values found by Martisen *et al* [15] for BSA diffusivity through different kinds and concentrations of Na alginate gels ($3.3–17.9 \times 10^{-7}\ cm^2\ s^{-1}$).

In Figure 6(a) and (b), the concentration profiles obtained with the model are compared with the experimental data. The achieved results fit the experimental ones well although it is necessary to highlight the discrepancy after 10 h. The experimental profiles are concave even at 51 h, when the stationary state is assumed to have been reached a long time previously, and the model gives plane profiles after 10 h. For the earlier times, the model predicts a slightly slower protein penetration than that shown by the experimental data. The diffusion model employed is a simplification of the experimental data. The diffusion model employed is a simplification of the experimental complexities that have been mentioned and possible phenomena that are not taken into account, namely steric problems near the central part of the support, repulsive electrostatic forces between the negatively charged alginate gel and the protein molecules or between the protein molecules [15] and a non uniform distribution of the alginate structure [11,15] may explain the diffusion discrepancies between experimental and model data at the early and final steps.

Goodness of fit: The usual method for determining the goodness of fit is to calculate $\Sigma(y_i - y_i^a)^2/\sigma_i^2$, where y_i is the gross data, σ_i are the standard deviations of the error for each datum and y_i^a the values of the intensities predicted by the fitting function. If the random errors are assumed to follow a Gaussian distribution with zero mean and standard deviation σ_i, this Σ follows a chi-square distribution with $N - M$ degrees of freedom, N being the data number and M the fitting parameter number (two in our case). This is valid if the fitting function depends linearly on its parameters.

In this case, as was pointed out earlier, it is impossible to know the σ value in advance, but it may be estimated by means of the detail coefficients of the first level (local fluctuations) (see Table 1). If the probability of the fitting being correct is determined using these values, very low values are obtained ($\cong 10^{-15}$). Apart from Gaussian errors, deviations exist that may be assimilated as systematic, which makes difficult the fitting to a parabola, as suggested by the data.

The repeatability of the results may be tested by analysing results obtained in different directions at each time. If σ is not calculated using wavelets and the fitting is assumed to be good, this will give an estimation of the random

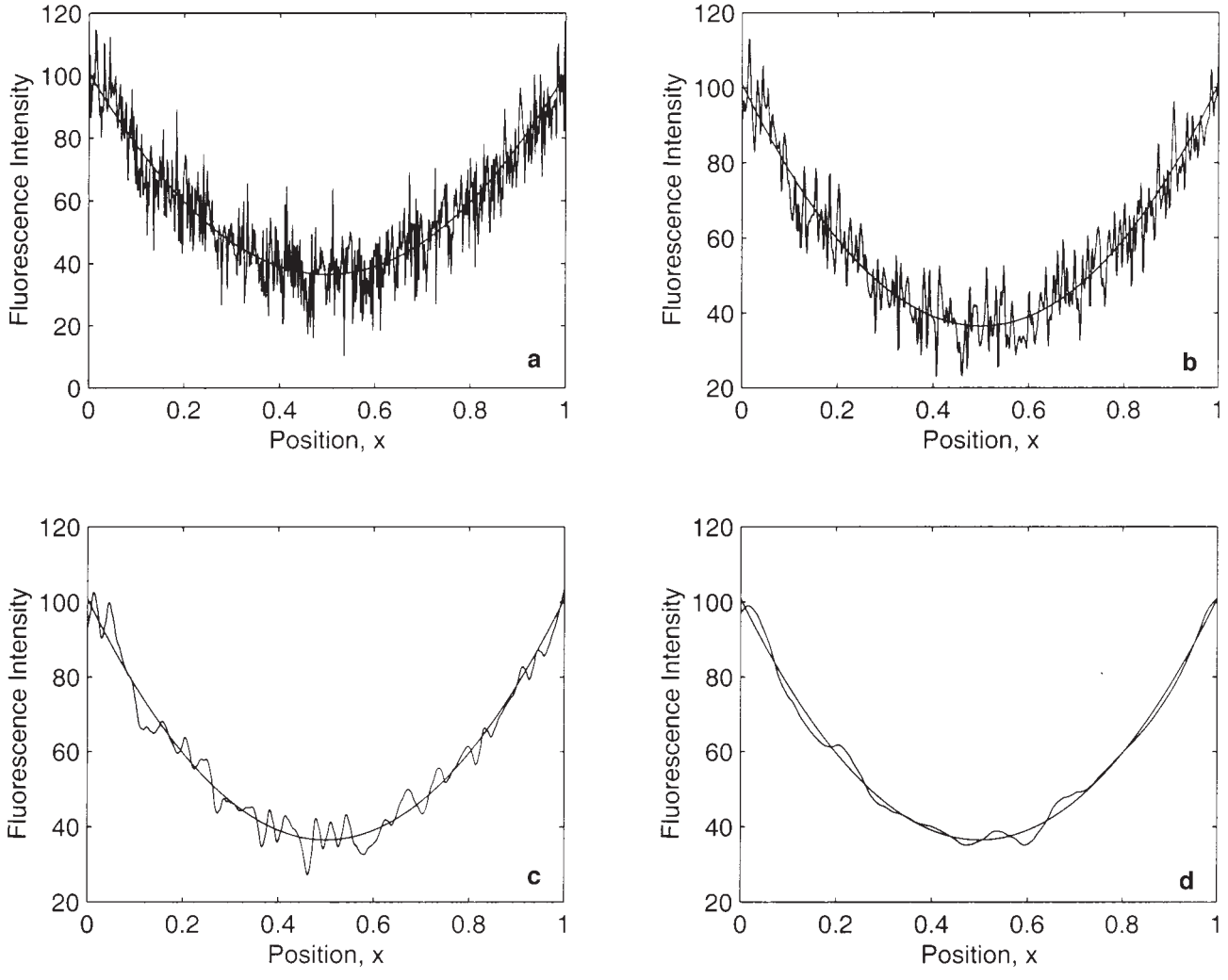

Figure 8 (a) Gaussian fluorescence intensity data simulated and added to the fitting parabola (diffusion time = 3 h). (b) Approximation with wavelets (level 1). (c) Approximation with wavelets (level 3). (d) Approximation with wavelets (level 5).

errors, $\sigma^2 = \Sigma(y_i - y_i^a)^2/(N-2)$. Using this estimation, the distribution of probabilities of the parameters *a* and *b* may be calculated and it is also possible to draw the outline of probabilities at a 99% level (Figure 7c and d), indicating that the results obtained in different directions are not coincident. This stands out clearly in the data for 5 h, whereas for 3 h, there are a number of intersection zones. An explanation for this is that the differences observed in the distinct directions are due to structural differences in the alginate, since the remaining errors should have affected all the directions in the same way.

If by σ_T we denote the standard deviation of the gross data with respect to the parabolic fitting, σ_T is different from the value of σ (random errors) calculated by means of wavelets. This implies the existence of systematic errors mentioned above and, assuming independence of both types of errors, we can calculate their standard deviation σ_S as $\sigma_S = (\sigma_T^2 - \sigma^2)^{1/2}$. These deviations ($\sigma_S$) are shown in Table 1 and hence, for each time and direction, we have an estimation of the deviation of the original data with regard to the parabola.

Comparison with Gaussian data: In order to illustrate the wavelets denoising technique, random data from the parabolic fitting corresponding to 3 h were generated, adding Gaussian errors with $\sigma = 10$ (Figure 8a), after cleaning up the data at different approximation levels. At the fifth level, the parabola is recovered with $\sigma = 2$ (Figure 8d). Denoising at levels one and three still leaves significant errors with values of $\sigma = 7$ and $\sigma = 3.5$ respectively (Figure 8b and c).

A final comment with respect to identifying zones of 'systematic' errors may be made comparing the real results with the simulated Gaussian data. Simulated data, adding Gaussian errors with standard deviation $\sigma = 10$, is shown in Figure 9(a), and it can be observed how practically all the data fall between $y \pm 2\sigma$, y being the fitting parabola. Gross data compared with the fitting parabola are shown in Figure 9b. Data outside of $y \pm 2\sigma$ correspond to zones where systematic deviations are more relevant with respect to the parabola plus the Gaussian fluctuations model. Thus, the more contaminated data may be eliminated.

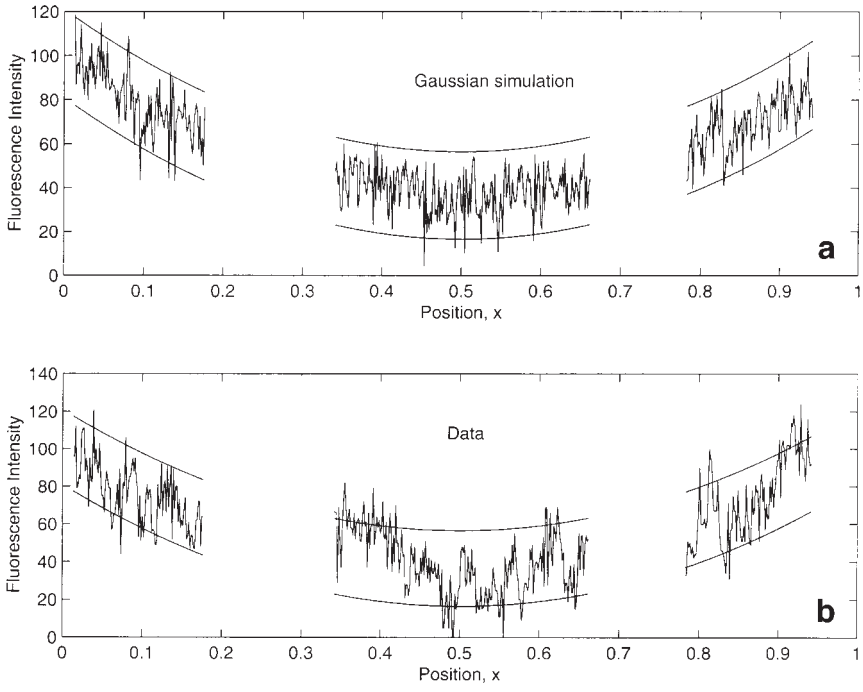

Figure 9 (a) Gaussian fluorescence intensity data simulated and added to the fitting parabola (diffusion time = 3 h) and fitting parabolic curves: $y + 2\sigma$; $y - 2\sigma$. (b) Gross fluorescence intensity data (diffusion time = 3 h) and fitting parabolic curves: $y + 2\sigma$; $y - 2\sigma$.

Conclusions

In order to understand the behaviour of immobilised cell systems in relation to modelling, it is necessary to ascertain the behaviour of substrates inside the support. By means of confocal microscopy, after labeling the protein with FITC, protein concentration profiles were obtained in an alginate support when the protein diffused from a liquid medium through the support. BSA, in spite of its high molecular weight, diffuses from the liquid medium through the alginate support, reaching the centre of the bead. Moreover, a diffusivity value, in accordance with other studies, was obtained by employing a diffusivity model.

Nevertheless, the experimental method presents a number of difficulties and measurement errors that lead to incomplete results together with some deviations, which implies their study and reconstruction. Hence, the data obtained were 'denoised' using wavelets analysis. Wavelets were also employed in order to infer the goodness of the parabolic models to which the results were fitted. Finally, a distinction has been made between Gaussian and systematic errors.

Symbols

a = parabola fitting parameter
b = parabola fitting parameter
C_{bs} = protein concentration in the liquid medium
$c_{j,k}$ = approximation coefficients (defined in Eqn 3)
C_s = protein concentration in the support
D_s = diffusivity of the protein in the support
$d_{j,k}$ = detail coefficients (defined in Eqn 4)
$\delta_{j,k}$ = detail coefficients after denoising
ε_L = porosity of the bed
f = general function
f_J = data constant in each subinterval
f_j = approximations at different levels
$\psi_{j,k}$ = wavelets (defined in Eqn 1)
ϕ = scaling function
$\phi_{j,k}$ = scaling functions (defined in Eqn 2)
g_j = details at different levels
j = level of resolutions
J = number of levels of resolution
k = position index
K = mass transfer coefficient in the external film
λ = threshold
M = fitting parameter number
N = number of data
r = radial co-ordinate of the support (centre of the support; $r = 0$)
R = average radius of the spherical particles
σ = standard deviation of the random errors
σ_i = standard deviation of the error for each datum
σ_T = standard deviation of the gross data with respect to the parabolic fitting
σ_S = standard deviation of the systematic errors
t = time
x = position (center of the support; $x = 0.5$)
y = intensity of fluorescence
y_i = gross data
y_i^a = intensities predicted by the fitting function
ψ = mother wavelet
$\psi_{j,k}$ = wavelets (defined in Eqn 1)

References

1 Aldrouby A and M Unser. 1996. Wavelets in Medicine and Biology. CRC Press, Boca Raton, Florida.

2 Cachon R, P Molin and C Diviès. 1995. Modeling of continuous pH-stat stirred tank reactor with *Lactococcus lactis* ssp *lactis* bv *diacetylactis* immobilized in calcium alginate gel beads. Biotechnol Bioeng 47: 567–574.
3 Casson D and AN Emery. 1987. On the elimination of artefactual effects in assessing the structure of calcium alginate cell immobilization gels. Enzyme Microb Technol 9: 102–106.
4 Chen H, JR Swedlow, M Grote, JW Sedat and DA Agard. 1995. The collection, processing, and display of digital three-dimensional images of biological specimens. In: Handbook of Biological Confocal Microscopy (Pawley JB, ed), Plenum Press, New York.
5 Daubechies I. 1988. Orthonormal bases of compactly supported wavelets. Comm Pure Appl Math 41: 909.
6 Donoho DL and IM Johnstone. 1995. Ideal spatial adaptation via wavelet shrinkage. Biometrika 81: 425.
7 Hahn R, PM Schulz, C Schaupp and A Jungbauer. 1998. Bovine whey fractionation based on cation-exchange chromatography. J Chromatogr A 795: 277–287.
8 Holmes K and BJ Fowlkes. Preparation of cells and reagents for flow cytometry. In: Current Protocols in Immunology (JE Coligan, AM Kruisbeek, DH Margulies, EM Shevach, eds), pp 5.3.5–5.3.6, USA.
9 Jawerth B and W Sweldens. 1994. An overview of wavelet based multiresolution analysis. SIAM review 36: 377.
10 Kaiser G. 1994. A Friendly Guide to Wavelets. Birkhäuser, Boston.
11 Khun RH, SW Peretti and DF Ollis. 1991. Microfluimetric analysis of spatial and temporal patterns of immobilized cell growth. Biotechnol Bioeng 38: 340–352.
12 Laca A, C Quirós, LA García and M Díaz. 1998. Modelling and description of internal profiles in immobilized cells systems. Biochem Eng J 1: 225–232.
13 Lowry OH, NJ Rosebrough and RJ Randall. 1951. Protein measurement with the Folin phenol reagent. J Biol Chem 193: 265–275.
14 Martínez-Nistal A, A Sampedro and M Matsuguchi. 1995. Introducción a la microscopía láser confocal. In: Técnicas de Fluorescencia en Microscopía y Citometría, pp 15–30. Publications Service of University of Oviedo, Oviedo.
15 Martinsen A, I Storrø and G Skjåk-Bræk. 1992. Alginate as immobilization material: III. Diffusional properties. Biotechnol Bioeng 39: 186–194.
16 Misiti M, Y Misiti, G Oppenheim and JM Poggi. 1996. Matlab Wavelet Toolbox User's Guide. The Math Works Inc, Natick, MA, USA.
17 Monbouquette HG, GD Sayles and DF Ollis. 1990. Immobilized cell biocatalyst activation and pseudo-steady-state behavior: model and experiment. Biotechnol Bioeng 35: 609–629.
18 Ogden RT. 1997. Essential Wavelets for Statistical Applications and Data Analysis. Birkhäuser, Boston.
19 ∅yaas J, I Storrø, H Svendsen and DW Levine. 1995. The effective diffusion coefficient and the distribution constant for small molecules in calcium-alginate gel beads. Biotechnol Bioeng 47:492–500.
20 Quirós C, LA García and M Díaz. 1996. The evolution of the structure of calcium alginate beads and cell leakage during protease production. Process Biochem 31: 813–822.
21 Sanz JL, F Argüeso, L Cayon, E Martínez-González, RB Barreiro and L Toffolatti. Wavelets applied to cosmic microwave background maps: a multiresolution analysis for denoising. Proceeding of the MPA/ESO Cosmology Conference, 2–7 August 1998, Garching, Germany. Evolution of large scale: from recombination to Garching (in press).
22 Scragg AH *et al* (eds). 1988. Biotechnology for Engineers. Ellis Horwood, New York.
23 Shoichet MS, RH Li and ML White. 1996. Stability of hydrogels used in cell encapsulation: an in vitro comparison of alginate and agarose. Biotechnol Bioeng 50: 374–381.
24 Tanaka H, M Matsumura and IA Veliky. 1984. Diffusion characteristics of substrates in ca-alginate gel beads. Biotechnol Bioeng XXVI: 53–58.
25 Vílchez MJ, J Vigara, I Garbayo and C Vílchez. 1997. Electron microscopic studies on immobilized growing *Chlamydomonas reinhardtii* cells. Enzyme Microb Technol 21: 45–47.
26 Vives C, C Casas, F Gòdia and C Solà. 1993. Determination of the intrinsic fermentation kinetics of *Saccharomyces cerevisiae* cells immobilized in Ca-alginate beads and observation on their growth. Appl Microbiol Biotechnol 38: 467–472.
27 Vuillemard J-C, S Terré, S Benoit and J Amiot. 1988. Protease production by immobilized growing cells of *Serratia marcescens* and *Myxococcus xanthus* in calcium alginate beads. Appl Microbiol Biotechnol 27: 423–431.
28 Wijffels RH, CD de Gooijer, AW Schepers, EE Beuling, LF Mallée and J Tramper. 1995. Dynamic modelling of immobilized *Nitrosomonas europaea*: implementation of diffusion limitation over expanding microcolonies. Enzyme Microb Technol 17: 462–471.